# ELECTRONIC SUPPORTING INFORMATION

## 3D texturing of the air–water interface by biomimetic self-assembly.

Erik Bergendal,[1] Richard A. Campbell,[2,3] Georgia A. Pilkington,[1] Peter Müller-Buschbaum,[4,5] Mark W. Rutland,[*1,6]

[1]Department of Chemistry, School of Engineering Sciences in Chemistry, Biotechnology and Health, KTH Royal Institute of Technology, Drottning Kristinas väg 51, 100 44 Stockholm Sweden

[2]Institut Laue-Langevin, 71 avenue des Martyrs, 38042 Grenoble, France

[3]Division of Pharmacy and Optometry, University of Manchester, Manchester M21 9PT, UK.

[4]Physik-Department, Lehrstuhl für Funktionelle Materialen, Technische Universität München, James-Franck-Str.1, 85748 Garching, Germany

[5]Heinz Maier-Leibnitz Zentrum (MLZ), Technische Universität München, Lichtenbergstr. 1, 85748 Garching, Germany

[6]RISE Research Institutes of Sweden, Chemistry, Materials and Surfaces, Box 5607, SE-114 86 Stockholm, Sweden

# SUPPLEMENTARY DATA

**S1 Surface pressure–area isotherms of EA and 19-MEA**

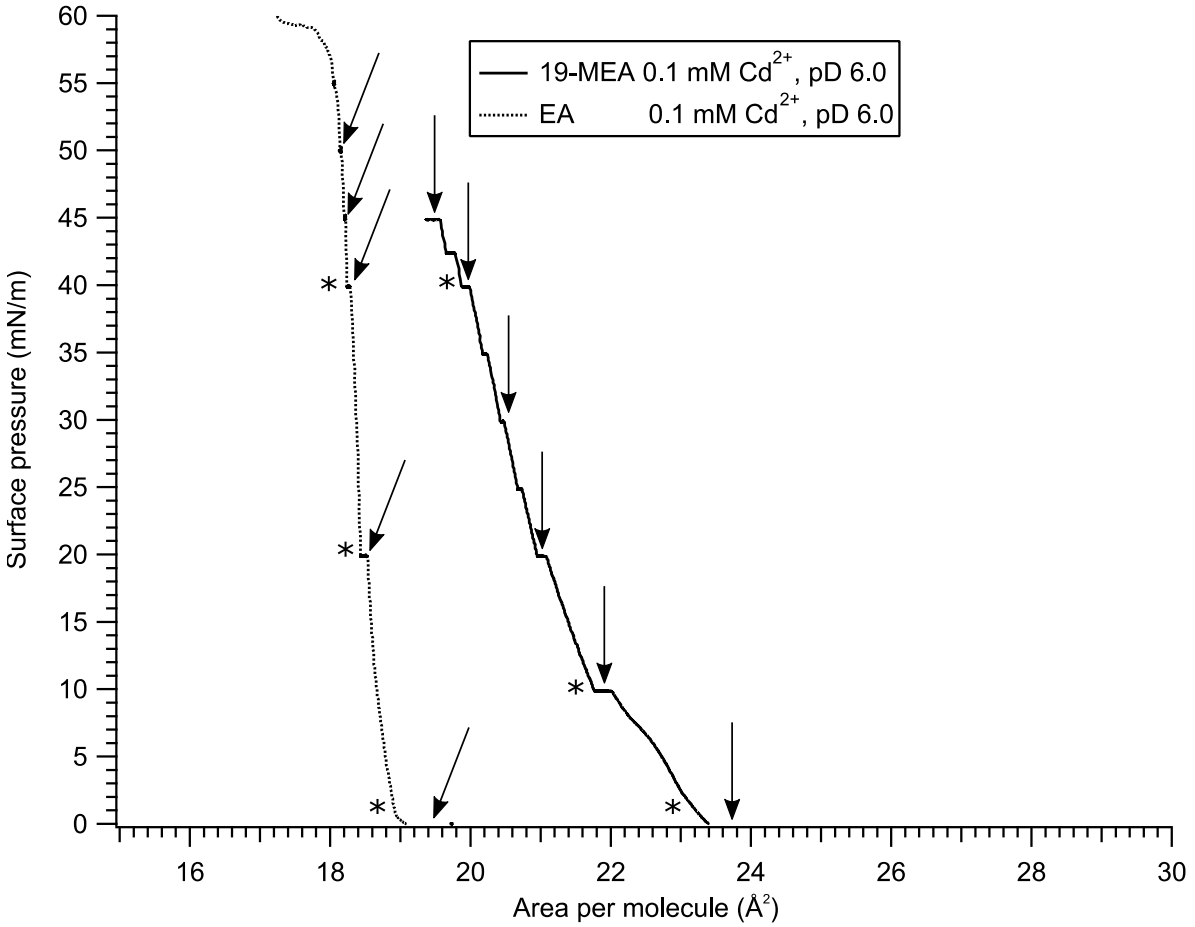


*S1 Pressure–Area isotherm of EA and 19-MEA collected during NR experiment. The isotherms have been shifted in area per molecule for comparison with Liljeblad et al.* [1]*. Stars and arrows show pressure at deposition and NR measurement, respectively. The decreased area per molecule during experiment is the result of continuous monolayer collapse when the surface pressure is held constant above its equilibrium spreading* pressure [2].

## S2 AFM characterisation of unbranched fatty acid monolayer

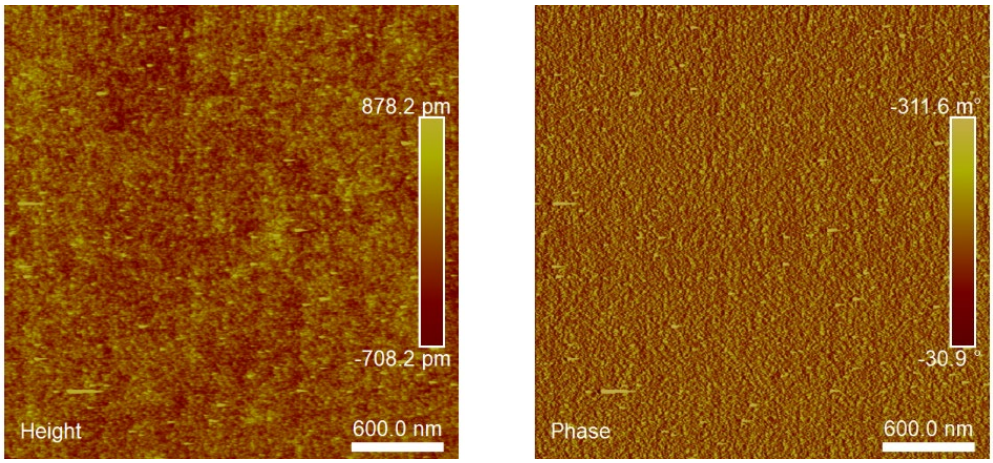


*S2 AFM height and phase image of deposited EA monolayer at 40 mN $m^{-1}$, showing a featureless morphology. Nanometer-sized multilayer patches are visible in the height image corresponding to trilayering seen in continuous monolayer collapse when held at constant pressure. In accordance with theory by Vollhardt [3].*

## S3 AFM character isation of unbranched fatty acid monolayer with height profile

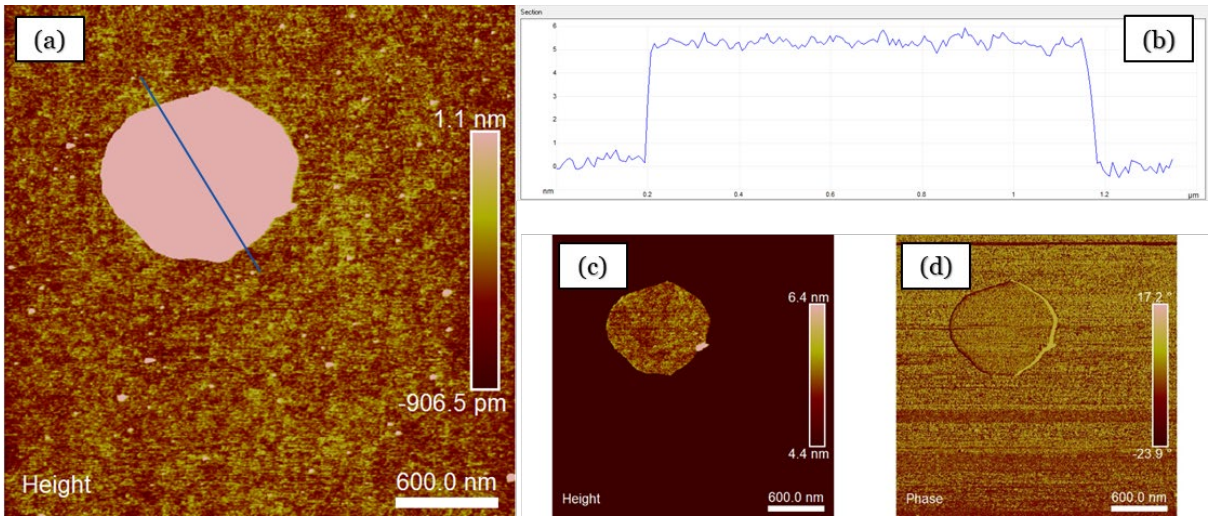


***S3. (a)** AFM height image of deposited monolayer of EA at 20 mN $m^{-1}$ showing a flat monolayer with a multilayer patch. With an extended chain length of ~25 Å this corresponds well to an expected trilayer as shown by the line profile in (b), which was taken over the particle. Image (c) shows the same image as (a) with a shifted height scale to emphasise the agreement in height profile of the monolayer and trilayer. Finally, (d) shows the phase image which confirms the same mechanical properties of the monolayer and the trilayer patch.*

## Neutron fitting parameters

Tables below shows fitting parameters used to generate fits for EA and 19-MEA as ST 1 and ST 2, respectively.

***ST 1.*** *Parameters used to fit NR data of EA using a two-layer model. *These parameters are fitted but constained to be equal. †These parameters where fitted against a neat $D_2O$ buffer subphase.*

| Model parameter | 0 mN $m^{-1}$ | 20 mN $m^{-1}$ | 40 mN $m^{-1}$ | 45 mN $m^{-1}$ | 50 mN $m^{-1}$ | free D2O surface |
|---|---|---|---|---|---|---|
| thickness tail (Å) | 23.9 | 25.5 | 25.5 | 25.5 | 25.5 | |
| thickness headgroup (Å) | 4.5 | 4.5 | 4.5 | 4.5 | 4.5 | |
| | | | | | | |
| SLD tail (x$10^{-6}$ Å$^2$) | -0.36 | -0.36 | -0.36 | -0.36 | -0.36 | |
| SLD headgroup (x$10^{-6}$ Å$^2$) | 4.7 | 4.7 | 4.7 | 4.7 | 4.7 | |
| SLD backing (x$10^{-6}$ Å$^2$) | 6.357 | 6.357 | 6.357 | 6.357 | 6.357 | 6.357† |
| | | | | | | |
| solvent penetration % | 33 | 33 | 33 | 33 | 33 | |
| | | | | | | |
| roughness tail (Å)* | 2.8 | 2.3 | 2.9 | 3.2 | 3.4 | |
| roughness headgroup (Å)* | 2.8 | 2.3 | 2.9 | 3.2 | 3.4 | |
| roughness backing (Å)* | 2.8 | 2.3 | 2.9 | 3.2 | 3.4 | 2.83† |
| **BACKGROUND** | | | | | | |
| 3.8E-7† | | | | | | |
| **SCALE** | | | | | | |
| 1 | | | | | | |

***ST 2.*** *Parameters used to fit NR data of 19-MEA using a two-layer model. *These parameters are fitted but constained to be equal. †These parameters where fitted against a neat $D_2O$ buffer subphase.*

| Model parameter | 0 mN $m^{-1}$ | 10 mN $m^{-1}$ | 20 mN $m^{-1}$ | 30 mN $m^{-1}$ | 40 mN $m^{-1}$ | 45 mN $m^{-1}$ | free $D_2O$ surface |
|---|---|---|---|---|---|---|---|
| thickness tail (Å) | 19.5 | 21 | 22.5 | 23.5 | 25 | 25.5 | |
| thickness headgroup (Å) | 4.5 | 4.5 | 4.5 | 4.5 | 4.5 | 4.5 | |
| | | | | | | | |
| SLD tail (x$10^{-6}$ Å$^2$) | -0.36 | -0.36 | -0.36 | -0.36 | -0.36 | -0.36 | |
| SLD headgroup (x$10^{-6}$ Å$^2$) | 4.7 | 4.7 | 4.7 | 4.7 | 4.7 | 4.7 | |
| SLD backing (x$10^{-6}$ Å$^2$) | 6.357 | 6.357 | 6.357 | 6.357 | 6.357 | 6.357 | 6.357† |
| | | | | | | | |
| solvent penetration % | 33 | 33 | 33 | 33 | 33 | 33 | |
| | | | | | | | |
| roughness tail (Å)* | 2.8 | 4.2 | 5.5 | 7.0 | 9.6 | 11.5 | |
| roughness headgroup (Å)* | 2.8 | 4.2 | 5.5 | 7.0 | 9.6 | 11.5 | |
| roughness backing (Å)* | 2.8 | 4.2 | 5.5 | 7.0 | 9.6 | 11.5 | 2.83† |
| **BACKGROUND** | | | | | | | |
| 3.8E-7† | | | | | | | |
| **SCALE** | | | | | | | |
| 1 | | | | | | | |

## SUPPLEMENTARY METHODS

### Fitting procedures: two-layer and slicing model

In the fitting procedure reffered to as Approach 1 in the main text, the carboxylic acid head group and the hydrocarbon tail of the fatty acids are divided into separate layers. In addition, the headgroup layer is in contact with the a water ($D_2O$) backing, and the tail group is in contact with an air backing. The headgroup and tail SLDs are calculated from molecular dimensions. The thickness of the headgroup is calculated from surface excess measurments, and estimated to that of EA, also for 19-MEA, as this would represent maximum compression of the monolayer. Due to the low sensitivity of neutron to the aliphatic chain, the 19-MEA chain length was assumed to the extended chain length at the highest surface pressure and estimated to vary linearly with reduced molecular area. This estimation of the chain length agrees with the present data, and will be regarded as satisfactory for the purpose of this article. However, to receive a better estimation of the chain length it would be necessary to use a different contrast variation (deuterated chains), or use a probe more sensitive to hydrocarbon scattering (X-rays). The solvent penetration provides the relationship between the volume fraction of the headgroup and aliphatic tail of one molecule, and describes how much of the headgroup layer will be occupied by the underlaying solvent. At each interface (air–tails, tails–headgroups, and headgroups–water), a roughness parameter is added to account for capillary wave roughness in addition to the texturing of the monolayer (and the underlaying water). The only parameter used to fit the data using Approach 1, is the roughness parameter. This parameter is constrained to be identical for the three interfaces.

Approach 1 uses Motofit to generate a reflectivity curve using Equation 2 from the main text, and a SLD-profile using Equation 3. In Approach 2, the SLD-profile generated by Approach 1, was sliced into 30 slices of 3 Å thickness each. This provided an array of SLD-values corresponding to the average SLD-value at a certain distance from the interface, as modelled by Approach 1. These values were then imported into Motofit as 30 layers of 3 Å thickness, with no interfacial roughness, to generate a *new* reflectivity curve corresponding to reflectivity data using Equation 2. Additionally, a SLD-profile was generated as a step function to the newly loaded data, using Equation 3. Consequently, the SLD-profile and the curve corresponding to the reflectivity data were generated separately.

## SUPPLEMENTARY DISUSSION

### S4 Roughness parameter in relation to capillary wave roughness

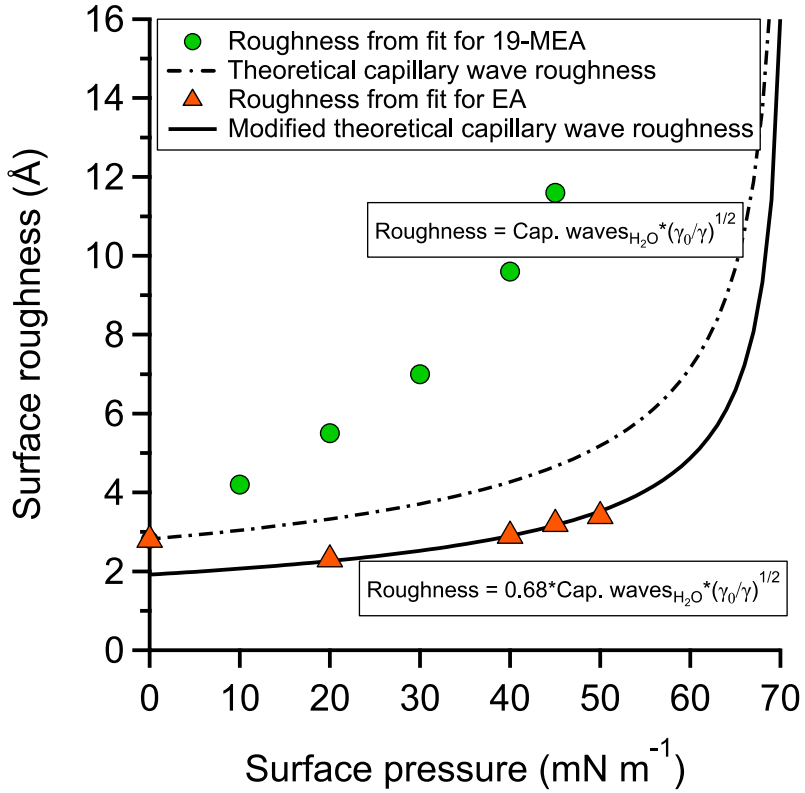


***S4**. Variation of the surface roughness used to fit experimental NR data for 19-MEA (green circles) and EA (orange triangles) shown together with the theoretically expected increase in surface roughness due to thermally excited capillary waves of water (dashed line) with decreasing surface tension. Additionally, a modified version of the theoretical capillary wave roughness is shown (solid line) with a shift in surface roughness. The theoretical capillary wave roughness describes how the surface roughness perceived as thermally excited capillary waves changes as a function of surface tension, $\gamma$, where $\gamma_0$ is the surface tension of a neat water surface.*

Figure S4 shows the same data as Figure 4 in the article, with the addition of a shifted theoretical line for capillary waves. This shifted fit for thermally excited capillary waves overlap with the experimental fits for surface roughness for EA. This increase in surface pressure after an initial decrease (due to monolayer rigidity as the monolayer reaches a solid phase) is in agreement with what has been previously observed for behenic acid monolayers studied with X-ray reflectometry [4]. Any attempts of a similar fit to the roughness for 19-MEA, yielded unsatisfactory results.

**Estimation of number of fatty acid molecules per 19-MEA surface domain**

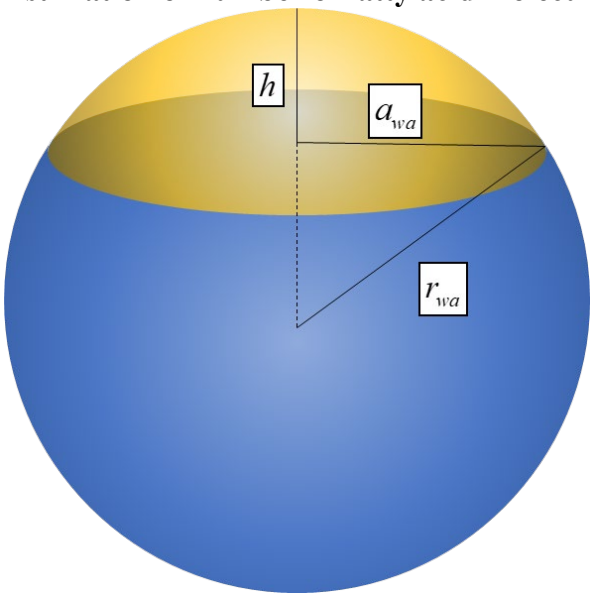


***S5.*** *Schematic representation of a spherical cap with parameters used to estimate the fatty acid coverage.*

A calculation of the number of molecules on a spherical cap is based on the radius of each aggregate extracted from AFM-images of deposited monolayers. This method yields 9575 molecules per aggregate employing a base radius of 250 Å and a cap height of 11.5 Å.

$$N_{MEA} = \frac{A_{cap}}{A_{EA}}$$

$$N_{MEA} = \frac{\pi\left(a_{wa}^2 + h^2\right)}{A_{EA}}$$

$a_{wa}$ – base radius of spherical cap
$h$ – height of spherical cap

The radius of curvature of the sphere can be calculated if the cap radius and height are known.

$$r_{wa} = \frac{\left(a_{wa}^2 + h^2\right)}{2h}$$

$r_{wa}$ – radius of curvature of spherical cap

The radius of curvature can be calculated using molecular parameters as described by reference 1:

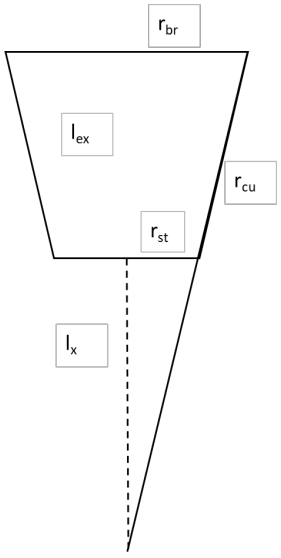


$$l_x = \frac{l_{ex}}{\left(\frac{r_{br}}{r_{st}} - 1\right)}$$

$$r_{cu} = \sqrt{\left(l_{ex} + l_x\right)^2 + r_{br}^2}$$

$$r_{wa} = r_{cu} - l_{ex}$$

where $r_{br}$ and $r_{st}$ is the radius of the branched and straight chain radius, respectively, estimated from isotherm data at a desired surface pressure. An estimation based on reference 1 used the area per molecule values for EA and 19-MEA of 18.7 Å$^2$ and 19.1 Å$^2$, respectively, extracted from a surface pressure of 45 mN m$^{-1}$. The extended chain length was estimated to 25.6 Å for a C19 hydrocarbon chain, excluding the headgroup carbon.

**Gravitation energy requirement for spherical cap formation**

In the supporting information of reference 1, an expression for the gravitational penanlty for lifting the water contained in a spherical cap was estimated. With a correction to the expression for the center of gravity, the gravitational energy can be summarised, simplified, and estimated as follows

$$\left.\begin{aligned} E_g &= mgz \\ m &= \rho V \end{aligned}\right\} E_g = \rho V g z \ \left(\mathrm{J}\right)$$

$$z = \frac{3\left(2r_{wa} - h\right)^2}{4\left(3r_{wa} - h\right)} \ \left(m\right)$$

$$V = \pi h^2 \left(r_{wa} - \frac{h}{3}\right) \ \left(\mathrm{m}^3\right)$$

$$E_g = \rho g \pi \frac{h^2}{4}\left(2r_{wa} - h^2\right) \ \left(\mathrm{J}\right)$$

$$E_g = 4.48^{-21} \ \left(\mathrm{J}\right)$$

$$E_g \approx 1.1 \ \mathrm{kT}$$

where $z$ is the centre of mass of the volume $V$ of water in the spherical cap. The estimated energy penalty is close to the thermal energy, as could be expected from a soft-matter system.

This can be related to an estimated energy penalty of hydrocarbon–water contact from domain edges. The contact area energy penalty is estimated to 104.6 J $mol^{-1}Å^{-2}$ [5]. Applying this to one spherical cap the energy penalty can be estimated as

$$E_{w/MEA} = \frac{25 \cdot 4.184 N_{MEA} A_{w/o}}{6.022 \cdot 10^{23}} \ \left(\mathrm{J}\right)$$

$$E_{w/MEA} = 1.74 \cdot 10^{-21} N_{MEA} A_{w/o} \ \left(\mathrm{J}\right)$$

$$E_{w/MEA} = 1.74 \cdot 10^{-21} N_{MEA} \pi l_{ex} \left(l_{ex} + 2a_{wa}\right) \ \left(\mathrm{J}\right)$$

$$E_{w/MEA} = 3.41^{-19} \ \left(\mathrm{J}\right)$$

$$E_{w/MEA} \approx 83 \ \mathrm{kT}$$

This shows that the hydrocarbon–water contact energy exceeds the expected gravitational penetly for lifting the water of the spherical caps by almost two orders of magnitute.

## SUPPLEMENTARY REFERENCES


1 J. F. D. Liljeblad, E. Tyrode, E. Thormann, A.-C. Dublanchet, G. Luengo, C. Magnus Johnson and M. W. Rutland, *Phys. Chem. Chem. Phys.*, 2014, **16**, 17869–17882.

2 P. M. Claesson and J. M. Berg, *Thin Solid Films*, 1989, **176**, 157–164.

3 D. Vollhardt, *Adv. Colloid Interface Sci.*, 2006, **123–126**, 173–188.

4 J. Daillant, L. Bosio, J. J. Benattar and J. Meunier, *Eur. Lett*, 1989, **8**, 453–458.

5 J. A. Reynolds, D. B. Gilbert and C. Tanford, *Proc. Natl. Acad. Sci.*, 1974, **71**, 2925–2927.